LC–DET–2001–006
January 12, 2001

Development of a TPC with GEM readout

Ties Behnke, Markus Hamann, Markus Schumacher

DESY

Abstract

We have studied a Time Projection Chamber (TPC) equipped with GEM (Gas Electron Multiplier) readout. The measurements have been performed with cosmic muons. Our studies comprise fundamental properties of the GEM readout: Besides the determination of the signal to noise ratio and the testing of the gain uniformity we have investigated the effective gain as a function of the voltages across the GEMs and as a function of the external fields. The exponential gain dependence on the GEM voltages as well as transfer processes and changes in the charge collection efficiency have been observed. Furthermore we have studied the resolution in time, which in our case is equivalent to the z resolution.

1 Introduction

A Time Projection Chamber (TPC, [1]) is proposed to be the main tracking device for the detector at the TESLA collider.
Our purpose is to study the TPC readout using Gas Electron Multipliers (GEMs, [2]) instead of wire chambers used conventionally to produce the gas amplification that is necessary to readout the signal. GEMs offer several advantages: $\vec{E} \times \vec{B}$ effects degrading the spatial resolution do not occur and the amount of required material in the end cap is low because there is no wire tension; ion feedback into the drift volume leading to field distortion is naturally suppressed to a level of a few percent and due to the absence of ion tails in the signal the use of GEMs improves the intrinsic two track resolution [3]. A TPC originally built as a prototype for the ALEPH TPC [4] is at our disposal. The former readout end plate has been replaced by a new one equipped with GEMs.

2 TPC setup

Figure 1 shows a schematic picture of our setup. It is divided into four main parts: the field cage, the GEM module, the trigger and the readout electronics. Cosmic muons are used as ionising particles.

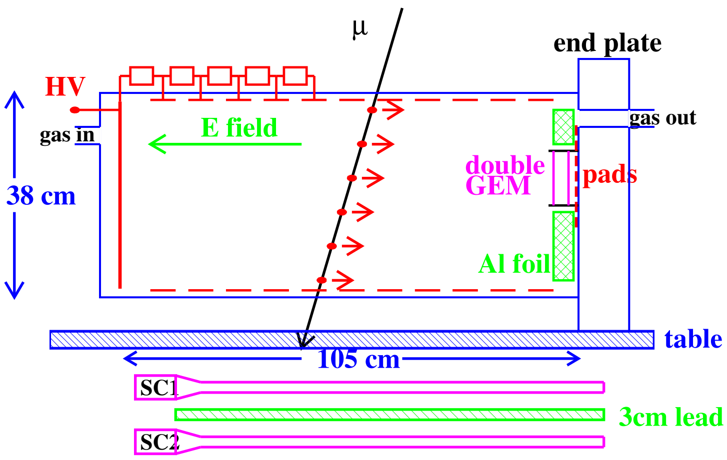

Figure 1: *Schematic picture of the setup*

2.1 Field Cage

The field cage has a length of 105 cm, an inner diameter of 38 cm and is made out of *Rohacell* surrounded by a copper layer which is grounded. The homogeneous

drift field is produced by 100 equipotential rings realized by copper strips of a width of 0.8 cm. The rings are connected in series via 1 MΩ resistor. The high voltage (HV) applied to the field cage can be adjusted up to 22 MV resulting in a drift field of about 210 V/cm.
The volume of the field cage is filled with the drift gas, which is a mixture of 93 % argon, 2 % carbon dioxide and 5 % methane.

2.2 GEM Module

The end plate contains four rows of readout pads consisting of eight strips each, but only one row is covered by GEMs (figure 2). The strips have a size of 5 cm × 5 mm and are aligned horizontally among one another, leaving a pitch of 6 mm. A double GEM structure is used to perform the gas amplification (figure 3). The GEM foils are mounted above the readout strips leaving a gap of 2 mm between GEM and strips (induction gap) and between the two GEMs, respectively (transfer gap). We call the GEM located directly above the readout pads GEM1 and the other one GEM2.
The foils were developed by the GDD Group at CERN. The holes have a double conical shape [5] with an outer diameter of 70 μm and an inner diameter of 55 μm. The pitch is 140 μm and each foil has a size of $10 \times 10\,\mathrm{cm}^2$.
Due to the applied electric fields in the induction gap (induction field), in the transfer gap (transfer field) and across each GEM, the potential on the upper side of GEM2 is about 1500 V. There is an aluminium foil on the same potential mounted around the GEMs in order to reduce the distortion of the drift field caused by the gradient to the ground potential to which the end plate is connected (see figure 3).

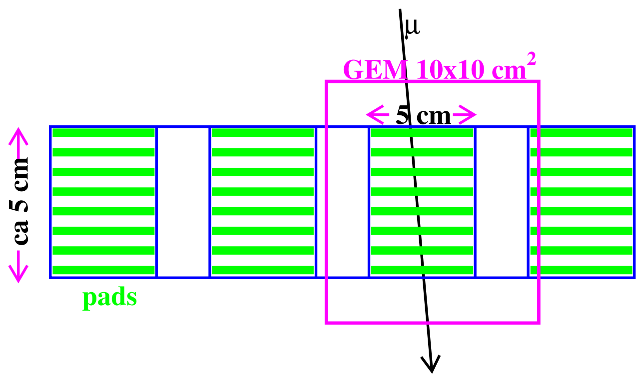

Figure 2: *Top view of the GEM readout*

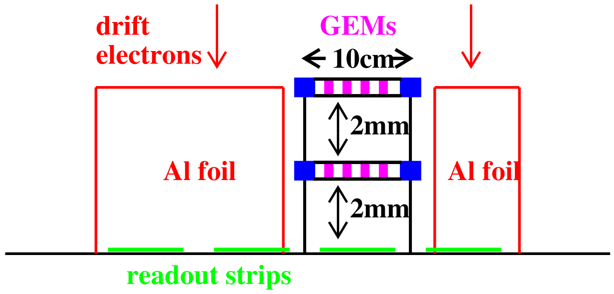

Figure 3: *Side view of the GEM readout*

2.3 Trigger

The reading out of the TPC data is started by a coincidence signal of two scintillators, opening a readout time interval of 50 μs. The scintillators have each a size of 20 cm $\times$ 80 cm and are located below the TPC, separated by a lead filter to stop low energetic muons (figure 1). Due to the alignment it is most probable that in case of a trigger signal the muon produces a signal on the pads.

2.4 Readout Electronics and Data Acquisition

The readout electronics consists of a standard ALEPH TPC charge integrating preamplifier for wire chambers with 16 channels [4], eight of them being connected to the pads that are covered by the GEMs. The preamplified signal is fed into an ADC module realized as the F6831 Time Projection Digitiser (TPD). The TPD includes a shaper and a Flash ADC (FADC) with a sampling rate of 11.4 MHz corresponding to time slices of 88 ns. Since the memory capacity is limited to 512 time samples, the maximum readout time for an event is $512 \times 88\,\mathrm{ns} \approx 45\,\mu\mathrm{s}$.
The TPD module is connected to a *Macintosh II* computer and the data is stored using *LabView* (including routines from the ALEPH TPC data acquisition). The readout system is driven by fastbus technology.

3 Measurements

We have performed a series of fundamental measurements, which will be described in the following. Unless otherwise noted, the measured values are averaged over the eight readout channels.

3.1 Signal to Noise

A good approximation for the noise N is given by the distribution of FADC counts of a run which is triggered externally by a pulse generator (see figure 4, left). The coincidence signal of the scintillators provides a veto to make sure no data taken corresponds to the signal of a muon. The signal (S) distribution is extracted from a "normal" run triggered by cosmic muons (figure 4, right). The particular mean values are divided leading to the estimate $S/N \geq 40$.
The peak in the signal distribution at approximately 850 counts has no physical meaning. It is due to charge pulses in the saturation region of the FADC.

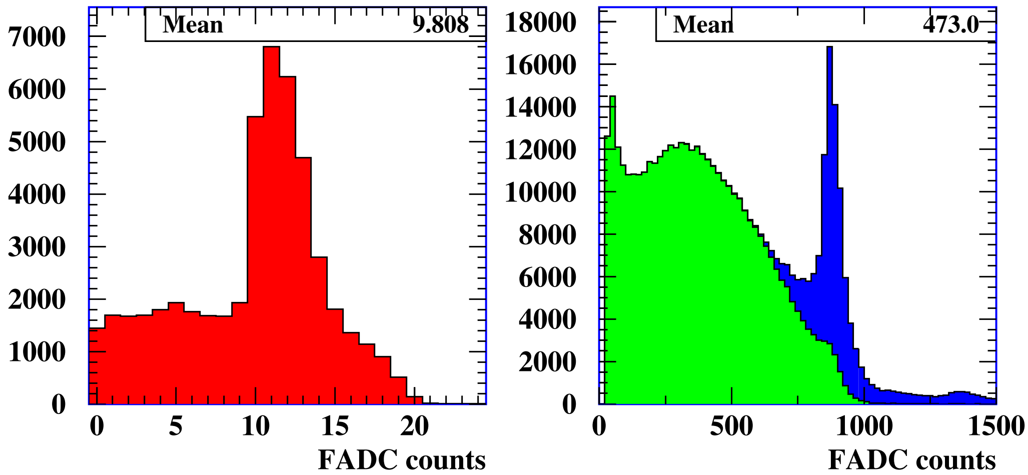

Figure 4: *Signal to noise ratio: left: noise N, right: signal S; $S/N \geq 40$.*

3.2 Effective gain

We are only able to measure the so called *effective* gain G_{eff} [5]. It can be written as the product of the *real* gain G_{real}, which is the intrinsic gain of the GEMs, and a field and geometry dependent factor T describing charge losses: $G_{eff} = T\,G_{real}$. As the number of electrons released by a minimum ionising particle for our gas mixture is approximately 100/cm [6], the effective gain is given by $G_{eff} = c\mathcal{N}/100e$, $\mathcal{N}$ being the number of FADC counts per pulse and c a proportionality constant.
For the investigation of the gain dependence on the applied electric fields we have performed three different series of measurements: the gain as a function of the GEM voltages, as a function of the induction and transfer field respectively and the gain dependence on the drift field.
Figure 5 shows the effective gain vs. the sum of the voltages of the two GEMs.

For each measurement series the voltage of one GEM is constant. The drift field is adjusted to $E_{drift} \approx 176\,\mathrm{V/cm}$. One can easily see a logarithmic dependence, which is in agreement with the other measurements [7]. For higher voltages the overall gain is in good approximation independent of the division of the gain between the two GEMs [3]. At values $U_{GEM1} + U_{GEM2} > 850\mathrm{V}$ we enter the region of saturation of the FADC.

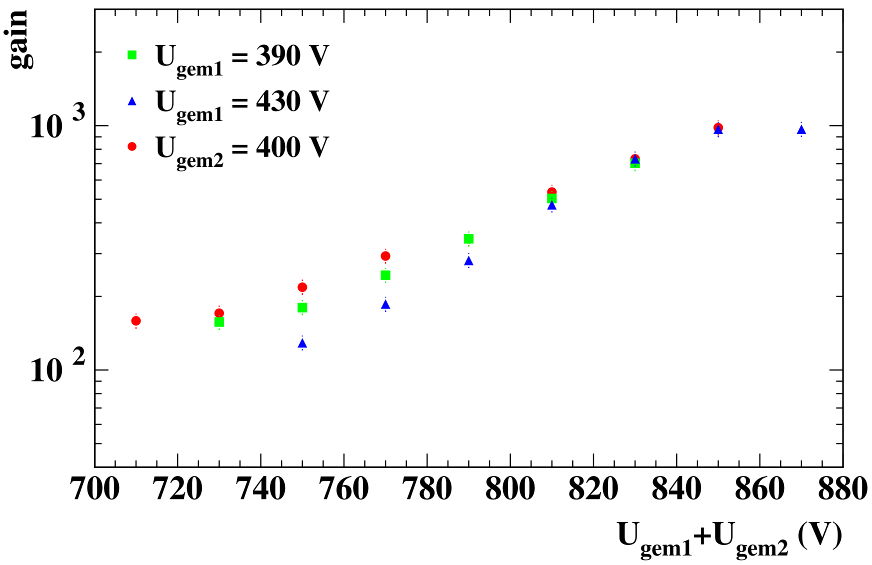

Figure 5: *Effective gain vs. GEM voltage*

The dependence on the induction and the transfer field is shown in figure 6. As in the previous measurement the drift field applied is $E_{drift} \approx 176\,\mathrm{V/cm}$. The GEM voltages are $U_{GEM1} = 430\,\mathrm{V}$ and $U_{GEM2} = 420\,\mathrm{V}$. In the case of variable induction field the transfer field is fixed to $U_{trans} = 1.09\,\mathrm{kV/cm}$, in the second case, i.e. variable transfer field, the induction field is adjusted to $U_{ind} = 1.25\,\mathrm{kV/cm}$. In both cases a rise of the gain with increasing field strength can be seen. Only at higher transfer fields (and a low induction field) the gain decreases slightly. Obviously the configuration of the transfer and induction field has a large impact on the parameter T changing the charge collection efficiency and the electrical transparency of the GEM foils. In the investigated region this leads to variations up to 20 % in the effective gain. Measurements done by other groups [5, 8] show similar results.
In the third measurement we have investigated the gain as a function of the drift field E_{drift} using a high and a low gas amplification (figure 7). The induction and transfer voltages are constant in each case. It can be seen that an increasing drift field leads to a rise of the effective gain. Using low gas amplification, i. e. low

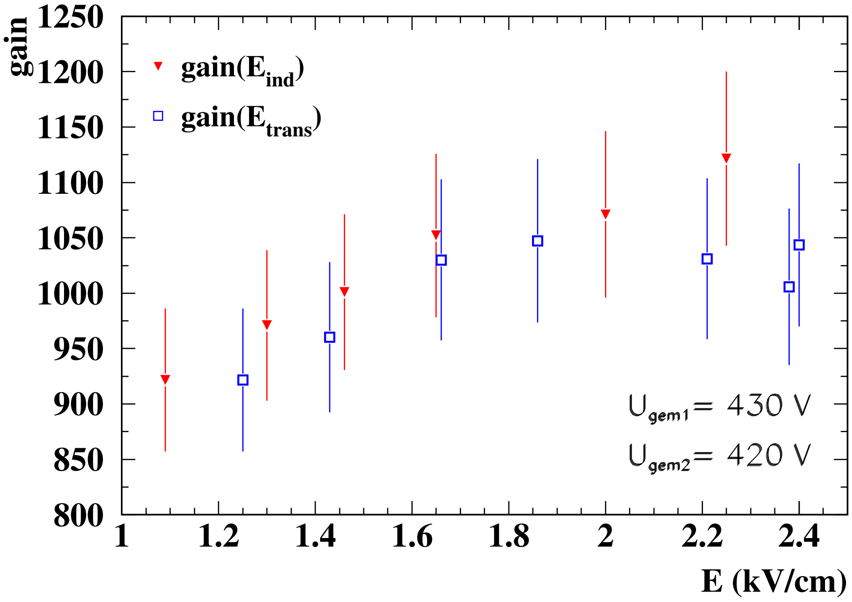

Figure 6: *Effective gain vs. induction and transfer field*

GEM voltages, this behaviour is moderate. But for high GEM voltages a strong rise is noticeable, which flattens out at $E_{drift} > 0.16\,\mathrm{kV/cm}$. Apparently the variation of the drift field changes the transparency and the charge collection efficiency of the readout system significantly. This leads to a change in the effective gain by a factor of ~ 5. The effect is large compared to the variation of the transfer and induction field and needs to be investigated further.
The gain shows a relatively uniform behaviour: a variation of less than 5 % with time (figure 8) and with the distance on the pad row, i. e. with the different channels (figure 9), can be seen. The gain variations in time have not been corrected for changes in the atmospheric pressure and temperature.

3.3 z resolution

In our setup the electrons drift parallel to the z axis, so that the z resolution σ_z is equivalent to the time resolution σ_t. This quantity is given by the width of the distribution $\sum(t - t_{fit})$. For each channel the time t of one pulse is determined using the weighting $t = (\sum t_i Q_i / \sum Q_i)$, Q_i being the measured charge in the time slice t_i with $1 \leq i \leq 10$. t_{fit} is the value obtained from a straight line χ^2 track fit.
Figure 10 shows the time resolution vs. the dip angle of the track whereas the reference axis is parallel to the pad row. A dependence of the measurement accuracy on the dip angle can be noticed. This is expected because with increasing dip angle pulses become longer in time and thus degrade the quality of the mea-

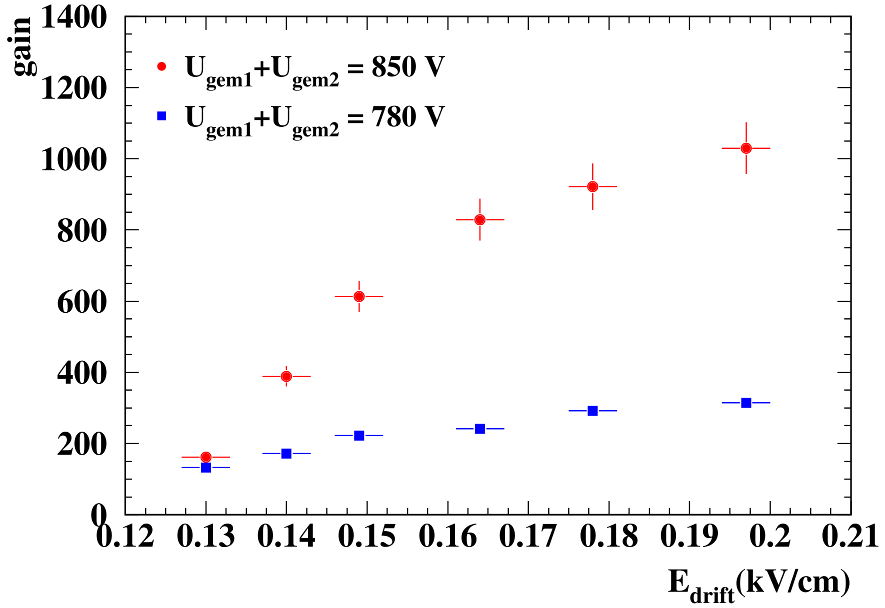

Figure 7: *Effective gain vs. drift field*

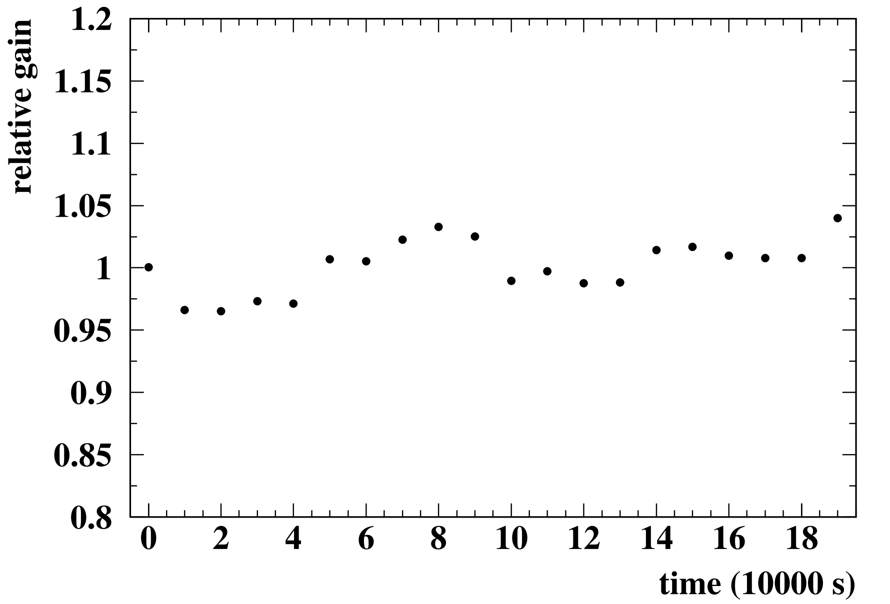

Figure 8: *Gain uniformity (1): relative gain w.r.t. the first bin vs. run time*

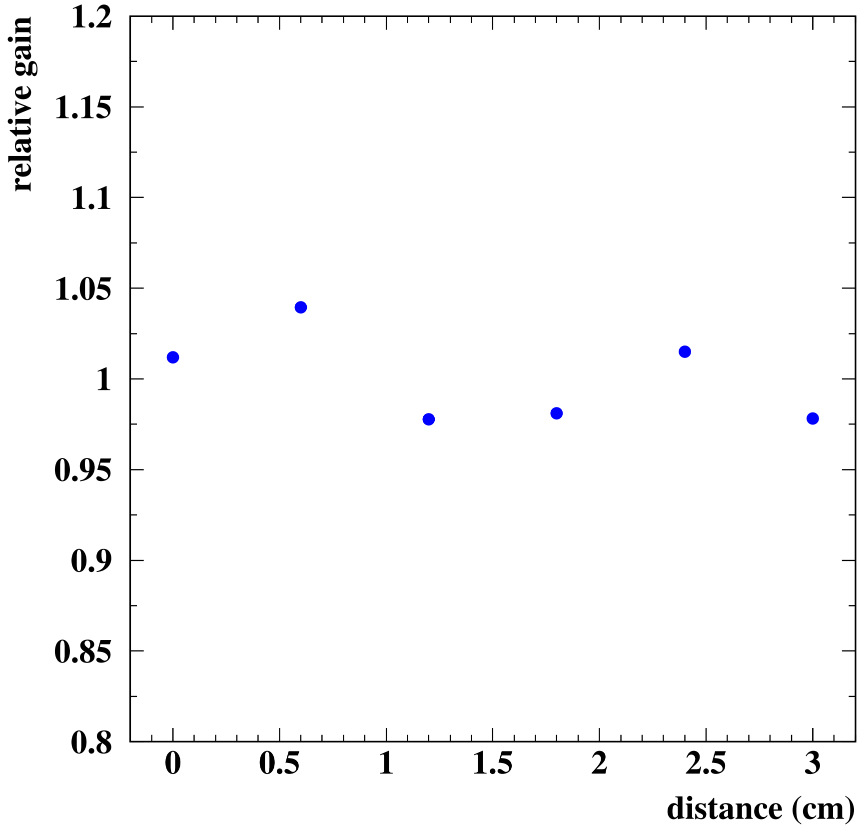

Figure 9: *Gain uniformity (2): relative vs. distance on the pad row*

surement [4].
Another effect degrading the resolution is the diffusion of the charge cloud which increases with increasing drift time (figure 11).
With the channel number the resolution varies within a few ns corresponding to a variation of about 10 % (see figure 12).
Assuming an electron drift velocity of $v_D \approx 4.5\,\mathrm{cm}/\mu\mathrm{s}$ [9] and a time resolution of $\sigma_t = 35\,\mathrm{ns}$ for tracks perpendicular to the z axis, the mean z resolution can be estimated to $\sigma_z \approx 1.6\,\mathrm{mm}$.

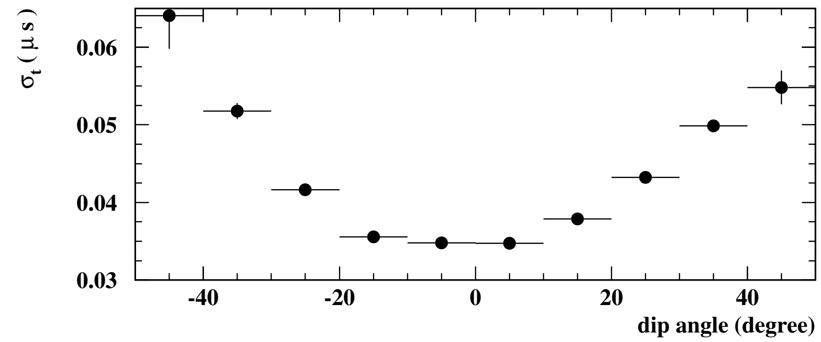

Figure 10: *Z resolution vs. dip angle*

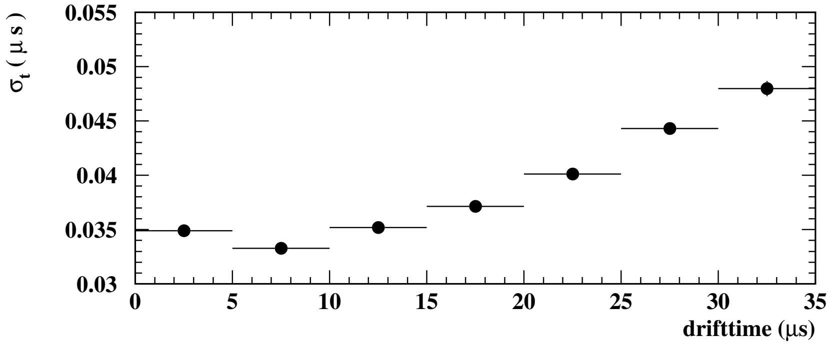

Figure 11: *Z resolution vs. drift time*

4 Summary and Outlook

For the study of the properties of the GEM readout of a TPC we have performed various measurements using cosmic muons:
The signal to noise ratio has been shown to be greater than 40 and the gain is highly uniform with variations being lower than 5 % (without corrections for changes in the atmospheric pressure and temperature). This is an encouraging

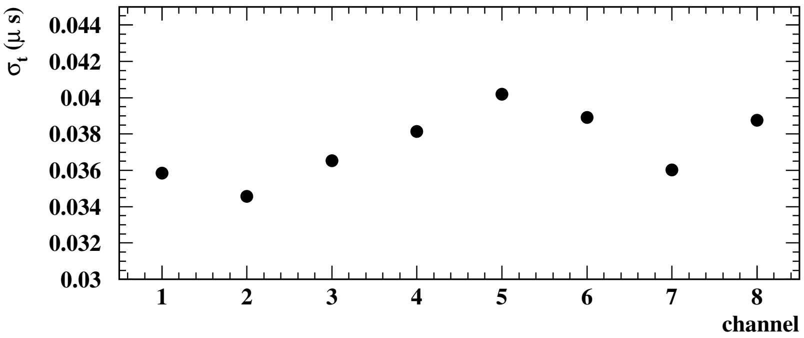

Figure 12: *Z resolution of each channel*

feature, which should allow $\mathrm{d}E/\mathrm{d}x$ measurements. Further gain measurements provide several fundamental information about the GEM performance in a TPC. The most important results are:

- the effective gain increases exponentially with the voltage applied across each GEM and is almost independent of the voltage sharing between GEMs;
- increasing the induction, transfer and drift field improves the the electron collection efficiency and the electrical transparency of the GEMs;
- some field configurations, i.e. low induction and high transfer field, lead to a decrease of the electrical transparency and the effective gain.

The z resolution is relatively uniform throughout the eight readout channels. The dependence on the dip angle of the muon track as well as the dependence on the drift time show the expected behaviour: The increasing pulse length with increasing dip angle and the diffusion of the charge cloud for longer drift times result in a lower z measurement accuracy.

Ongoing research will include an optimisation of the field configuration to achieve a larger effective gain. Two double GEM structures side by side as well as a larger number of readout channels will be installed, allowing 64 rectangular pads to provide information in z and $r\phi$. So real three dimensional space points and tracks can be reconstructed; point and two track resolution will be studied, including effects at the transition region of the two double GEM structures.
Although ion feedback is suppressed naturally, a small fraction of ions cannot be prevented from drifting into the drift volume. In a separate setup this effect will be investigated.

References

[1] D. R. Nygren, *The Time Projection Chamber: A new 4 pi detector for charged particles.*, PEP-0144, Proceedings, Pep Summer Study, Berkeley 1975, page 58-78.

[2] F. Sauli, Nucl. Instrum. and Meth. **A386** (1997) 531.

[3] F. Sauli, CERN–EP–TA1 Internal Report, July 29, 1999

[4] C. Bowdery (editor), *The Aleph Handbook 1995, Volume 1, Chapter V*, ISBN 92–9083–072–7

[5] S. Bachmann et al., CERN–EP/99–48

[6] F. Sauli, *Principles of operation of multiwire proportional and drift chambers*, May 3, 1977

[7] S. Bachmann et al., CERN–EP/2000–077

[8] M. Ziegler et al., hep–ex/0007007, July 4, 2000

[9] M. Gruwe, *Gas Studies for a TPC of a detector for the future linear collider TESLA*, LC-DET-1999-003-TESLA, Feb 1, 1999